

Characterising Multi-Pathogen Grapevine Dieback in Subtropical Australia: Field Symptomatology and Fungal Morphology Reveal Dominance of Botryosphaeriaceae and Phomopsis Species

Xingru Meng

The University of Queensland, Brisbane, Australia
rara481846778@gmail.com

Abstract. Grapevine trunk diseases in subtropical climates show complex patterns of multi-pathogen co-infection and spatial clustering, while current diagnosis still relies mainly on expert judgement with limited quantification and functional testing. This study investigated an 18-acre vineyard in south-eastern Queensland and used 7,440 vine records from 744 plots to build quantitative indices for symptoms and cross-section necrosis, followed by comprehensive characterisation of 46 fungal isolates through isolation, microscopy, physiological assays and greenhouse pathogenicity tests. Analyses identified three spatial disease regions, with wedge- and semi-ring-shaped necrosis strongly enriched in high-disease plots, and showed that Botryosphaeriaceae and Phomopsis groups dominated the pathogen community and had much higher composite pathogenicity indices than other fungi. Even without molecular data, the integrated pipeline of disease quantification, microscopic and physiological traits, pathogenicity testing and computational analysis allowed robust identification of dominant pathogen combinations in a subtropical vineyard and provided a methodological basis for regional risk assessment and targeted management.

Keywords: Grapevine trunk disease, Botryosphaeriaceae, Phomopsis, Pathogenicity test, Computational analysis

1. Introduction

Grapevine trunk diseases are recognised as key drivers of yield loss, fruit quality decline and premature vineyard removal, and their epidemics often unfold over many years, which makes them difficult to detect and manage in time [1]. In temperate and Mediterranean regions, previous studies have already described pathogen community structures, infection windows and management options in a systematic way, but in hot and humid subtropical areas where pruning cycles and rainfall events strongly overlap, quantitative research on multi-pathogen co-infection patterns remains limited. Traditional diagnosis relies mainly on visual assessment and a small number of isolations, without standardised disease indices, pathogenicity tests or multidimensional feature analysis, and thus links between field symptoms and specific pathogens remain blurred [2]. When molecular identification is

not yet routinely available, it is difficult to generate a robust pathogen evidence base for regional control strategies if morphology is not reinforced by microscopic, physiological and pathogenicity data [3]. Against this background, this study focuses on a subtropical vineyard in south-eastern Australia and combines quantitative field surveys, fungal isolation and microscopic-physiological characterisation, pathogenicity tests and R- and Python-based spatial and clustering analysis to describe patterns of multi-pathogen dieback and dominant pathogen communities, and to develop an operational integrated diagnostic framework under conditions where molecular data are not yet in place.

2. Literature review

2.1. Pathogen diversity and epidemiology of grapevine trunk diseases

Existing studies generally treat grapevine trunk diseases as pathogen complexes rather than single diseases, and Botryosphaeriaceae, Phomopsis, Eutypa and other groups show different dominance patterns and coexistence structures across climate zones and production systems [4]. Field and isolation studies have shown that a single vine often harbours multiple wood-inhabiting fungi, some of which are strongly pathogenic whereas others express pathogenicity only under stress, so pathogen communities are highly heterogeneous in both temporal and functional dimensions [5]. At the epidemiological level, pruning regimes, grafting practices, vine age structure, row orientation and drainage conditions jointly shape infection and dispersal processes, and some management practices can reduce infection windows while others unintentionally increase disease pressure by increasing wound frequency or prolonging wetness duration.

2.2. Diagnostic challenges under subtropical climatic conditions

In subtropical climates, high temperatures, intense rainfall and extreme storms act together and make grapevines more prone to wind damage, sunburn and root hypoxia, which can produce shoot dieback, leaf yellowing and trunk necrosis that closely resemble trunk disease symptoms [6]. Multi-pathogen co-infection further creates an “overlay effect”, in which wedge-shaped necrosis, ring-shaped necrosis, pruning-wound cankers and bud failure occur on the same vine, and this erodes the one-to-one indicative value of “typical symptoms” used in experience-based diagnosis [7]. Many field surveys use coarse ordinal scales or binary classes to describe disease status and therefore cannot capture continuous changes in symptom shape, necrosis pattern and severity.

2.3. Integrating morphology, microscopy and computational methods

Colony morphology and spore traits have long served as the starting point for identification of trunk disease pathogens, but even small changes in culture conditions and observation time can shift colour, texture and reproductive structures, and phenotypic overlap among species creates a substantial risk of misidentification [8]. Microscopic observations and physiological measurements partly address this problem, because different pathogens tend to show relatively stable functional differences in conidial morphology, attachment structures, optimum temperature, growth rate and enzyme activity profiles, which supports grouping them into functional types with distinct aggressiveness and ecological niches [9]. At the same time, computer vision and machine learning methods have been introduced into leaf disease image recognition and disease severity estimation, and spatial statistics and GIS are used to describe disease spread at vineyard and landscape scales,

but in trunk disease research many studies still stop at a molecular phylogenetic description of “who is present”.

3. Experimental methods

3.1. Vineyard characteristics and quantitative field survey design

An 18-acre vineyard in south-eastern Queensland with 62 rows and 12 panels per row (744 spatial units) served as the study site, with 10 vines randomly selected in each unit and cultivar, row ID and GPS coordinates recorded for every vine. Trunk, cordon and cane dieback were scored in the field on a 1–9 disease index using a tablet-based form, yielding 7,440 single-vine records with a vineyard-wide mean disease index of 4.3 and a standard deviation of 1.9. Plot-level disease indices were aggregated as a row–panel matrix in R using the *sf* and *ggplot2* packages to generate disease heatmaps, and k-means clustering with $k = 3$ was applied to define low-, medium- and high-disease regions, which subsequently guided the selection of plots and vines for pathogen isolation.

3.2. Fungal isolation, microscopic morphology and physiological characterisation

From each of the three disease clusters defined in 3.1, 10 plots were selected and three vines per plot were sampled, giving 90 vines in total; from each vine, 5–10 cm segments of trunk and cordon were cut, split longitudinally and 2×2 mm wood chips were excised from the interface between healthy and necrotic tissue. After surface sterilisation, chips were placed on 1/2 PDA amended with $0.1 \text{ g} \cdot \text{L}^{-1}$ streptomycin and incubated at 25°C in darkness for seven days, then morphologically distinct colonies from each sample were subcultured three times on PDA to obtain pure isolates, resulting in 46 stable strains with radial growth rates at 25°C ranging from 2.4 to $7.1 \text{ mm} \cdot \text{d}^{-1}$ [10]. Isolates were grown on PDA, MEA and Czapek media at 20, 25 and 30°C to measure growth rate, sclerotia formation and pigment production, and at least 50 conidia per isolate were measured under a light microscope for length, width and septation; all functional and morphological traits were assembled into a feature matrix for multivariate clustering and for selecting representative isolates for pathogenicity testing.

3.3. Pathogenicity tests

Clustering of the 46 isolates from 3.2 based on morphology and physiology yielded a *Botryosphaeriaceae* group (12 isolates), a *Phomopsis* group (9 isolates) and an “other” group (5 isolates), which were used for pathogenicity tests on one-year-old grape canes under greenhouse conditions with three inoculation points per cane, five canes per isolate and sterile PDA controls [11]. After 28 days, lesion lengths were measured and re-isolation attempted, and disease severity for each treatment was calculated with the disease severity index, as shown in Equation (1).

$$\text{DSI} = \frac{\sum_{i=1}^k r_i n_i}{9N} \times 100 \quad (1)$$

Where r_i is the i -th rating, n_i is the number of vines at that rating and N is the total number of vines; for each isolate j , a composite pathogenicity index as shown in Equation (2).

$$\text{PI}_j = \alpha \frac{L_j}{L_{\max}} + (1 - \alpha) \frac{P_j}{100} \quad (2)$$

Where L_j is mean lesion length, L_{\max} is the maximum mean lesion length across isolates, p_j is the re-isolation success rate and α was set to 0.6. Field-level DSI values, necrotic area percentages extracted from cross-section images and isolate feature data were combined in R and Python, principal component analysis and k-means clustering were used to jointly classify plots and isolates, and resulting feature vectors and cluster labels were used to define symptom-pathogen lineages.

4. Results

4.1. Spatial distribution of disease, symptom types and quantitative features

Trunk disease indices across the 744 plots ranged from 1 to 9 with a mean of 4.3 and a standard deviation of 1.9, producing a slightly right-skewed distribution in which low-, medium- and high-disease plots accounted for approximately 38.2%, 34.4% and 27.4% of the vineyard, respectively. k-means clustering on plot-level mean indices with $k = 3$ yielded low-, medium- and high-disease regions with mean DSI values (mean \pm SD) of 2.1 ± 0.6 , 4.6 ± 0.7 and 6.8 ± 0.8 , forming three relatively continuous bands located mainly on the lower southern slope, the central gentle slope and the upper northern slope. For 180 representative trunk cross-sections from these regions, ImageJ-based thresholding and area calculations indicated median necrotic wood proportions of 7.9%, 23.6% and 41.2% in low-, medium- and high-disease plots, respectively, with necrosis patterns shifting from predominantly band-like in low-disease plots to mixed bands and wedges in medium-disease plots and to mainly wedge- and semi-ring-shaped necrosis in high-disease plots; in Figure 1, a row-panel heatmap combined with a PCA biplot of symptom and necrosis metrics shows that the first two principal components explain 68.4% of the variance and that high-disease plots cluster in the same quadrant as high necrotic area, high wedge-type necrosis frequency and large DSI values.

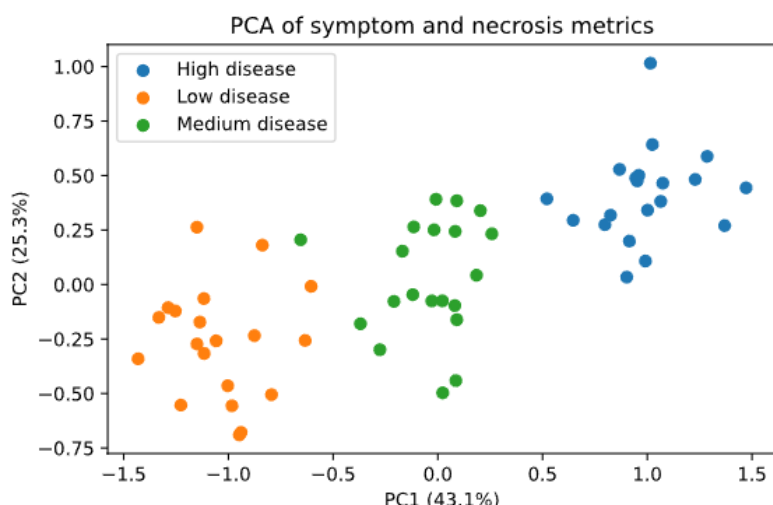


Figure 1. PCA of symptom and necrosis metrics across low-, medium- and high-disease plots

4.2. Composite traits and pathogenicity of dominant pathogen groups

Clustering of the 46 isolates based on morphological and physiological traits and PCA separated them into a Botryosphaeriaceae group (12 isolates), a Phomopsis group (9 isolates) and an “other” group (5 isolates), with the first two groups predominantly originating from medium- and high-disease plots and the third group mainly from low-disease plots. Greenhouse inoculation tests at 25 °C showed that the Botryosphaeriaceae group had a mean radial growth rate of $6.2 \pm 0.7 \text{ mm} \cdot \text{d}^{-1}$, a

mean lesion length of 32.4 ± 5.3 mm and a re-isolation success rate of 91.7%, whereas the *Phomopsis* group exhibited corresponding values of 4.8 ± 0.5 mm·d⁻¹, 24.7 ± 4.2 mm and 85.2%, and the “other” group only 3.1 ± 0.6 mm·d⁻¹, 8.9 ± 3.1 mm and 26.7%. Application of the composite pathogenicity index formula in 3.3 yielded median PI values of 0.81, 0.67 and 0.23 for the *Botryosphaeriaceae*, *Phomopsis* and “other” groups, respectively; Table 1 summarises these growth, lesion and pathogenicity metrics and shows that the two dominant groups combine higher physiological activity and pathogenicity with higher isolation frequencies from plots characterised by higher DSI values and higher proportions of wedge-type necrosis.

Table 1. Physiological and pathogenicity traits of three pathogen groups isolated from the subtropical vineyard

Group	Isolate count	Growth rate mm·d ⁻¹ (mean ± SD)	Lesion length mm (mean ± SD)	Re-isolation success (%)	PI median
<i>Botryosphaeriaceae</i>	12	6.2 ± 0.7	32.4 ± 5.3	91.7	0.81
<i>Phomopsis</i>	9	4.8 ± 0.5	24.7 ± 4.2	85.2	0.67
Other	5	3.1 ± 0.6	8.9 ± 3.1	26.7	0.23

5. Discussion

Findings indicate that trunk disease in the subtropical vineyard did not spread uniformly but formed three spatial clusters of low, medium and high disease that were shaped by topography and drainage, with disease index, necrotic area and wedge-type necrosis frequency showing a stable coupling. Fungal isolation and functional clustering showed that *Botryosphaeriaceae* and *Phomopsis* groups occurred most frequently in medium and high disease plots and displayed higher growth rates, longer lesions and higher re-isolation success than other fungi; composite pathogenicity indices correlated with plot DSI and wedge-type necrosis with coefficients of 0.62–0.74, supporting a central causal role in this vineyard. By embedding microscopic traits, physiological profiles and pathogenicity tests in a single analytical framework, the study strengthened morphology-based diagnosis and, through PCA and clustering, compressed complex symptom and multi-pathogen information into interpretable feature vectors, which prepares a suitable data structure for integration with future molecular phylogenetics and machine-learning models.

6. Conclusion

An integrated diagnostic framework for subtropical grapevine trunk disease was developed that combines quantitative field surveys, microscopic and physiological characterisation, pathogenicity tests and computational analysis, and that can identify dominant pathogen groups even in the absence of molecular typing. Clear spatial gradients of disease were detected, with high-disease plots associated with larger necrotic areas and wedge-type necrosis, and dominant pathogen communities composed of *Botryosphaeriaceae* and *Phomopsis* isolates with higher composite pathogenicity indices, while other fungi behaved mainly as weak or opportunistic taxa. Standardised disease indices, quantitative image analysis and multivariate clustering together yielded an operational symptom–pathogen profile under constrained resources and created a starting point for future work that will incorporate molecular data, expand temporal and spatial coverage and apply

machine-learning approaches to build regional early-warning and management decision-support systems.

References

- [1] DeKrey, David H., et al. "Grapevine trunk diseases of cold-hardy varieties grown in Northern Midwest vineyards coincide with canker fungi and winter injury." *Plos one* 17.6 (2022): e0269555.
- [2] Azevedo-Nogueira, Filipe, et al. "The road to molecular identification and detection of fungal grapevine trunk diseases." *Frontiers in plant science* 13 (2022): 960289.
- [3] Kraus, Christian, et al. "Minimal versus intensive: how the pruning intensity affects occurrence of grapevine leaf stripe disease, wood integrity, and the mycobiome in grapevine trunks." *Journal of Fungi* 8.3 (2022): 247.
- [4] Travadon, Renaud, et al. "Fungal species associated with grapevine trunk diseases in Washington wine grapes and California table grapes, with novelties in the genera Cadophora, Cytospora, and Sporocadus." *Frontiers in fungal biology* 3 (2022): 1018140.
- [5] Dewasme, Coralie, et al. "Long-term esca monitoring reveals disease impacts on fruit yield and wine quality." *Plant disease* 106.12 (2022): 3076-3082.
- [6] Billones-Baaijens, Regina, et al. "Molecular detection and identification of Diatrypaceous airborne spores in Australian vineyards revealed high species diversity between regions." *PloS One* 18.6 (2023): e0286738.
- [7] Adejoro, Damola O., et al. "Grapevines escaping trunk diseases in New Zealand vineyards have a distinct microbiome structure." *Frontiers in Microbiology* 14 (2023): 1231832.
- [8] Ji, Tao, et al. "Role of rain in the spore dispersal of fungal pathogens associated with grapevine trunk diseases." *Plant Disease* 108.4 (2024): 1041-1052.
- [9] Meza, Leticia, et al. "Grapevine pruning strategy affects trunk disease symptoms, wood pathobiome and mycobiome." *Phytopathologia Mediterranea* 63.1 (2024): 91-102.
- [10] Leal, Catarina, et al. "Exploring factors conditioning the expression of Botryosphaeria dieback in grapevine for integrated management of the disease." *Phytopathology®* 114.1 (2024): 21-34.
- [11] Moret, Florian, et al. "Physiological and developmental disturbances caused by Botryosphaeria dieback in the annual stems of grapevine." *Frontiers in Plant Science* 15 (2024): 1394821.